Evidence for oxygen-island formation on Al(111): Cluster-model theory and x-ray photoelectron spectroscopy

P. S. Bagus, C. R. Brundle, F. Illas,* F. Parmigiani,† and G. Polzonetti‡
IBM Research Division, Almaden Research Center, 650 Harry Road, San Jose, California 95120-6099
(Received 18 March 1991)

The O 1*s* x-ray photoelectron spectroscopy spectrum for Al(111)/O at 300 K shows two components whose behavior as a function of time and variation of detection angle are consistent with either (a) a surface species represented by the *higher* binding-energy (BE) component and a subsurface species represented by the *lower* BE component, or (b) small close-packed oxygen islands with the interior atoms represented by the *lower* BE component and the perimeter atoms by the *higher* BE component. We have modeled both situations using *ab initio* Hartree-Fock wave functions for clusters of Al and O atoms. For an O atom in a threefold site, it was found that a below-surface position gave a *higher* O 1*s* BE than an above-surface position, incompatible with interpretation (a). This change in the O 1*s* BE could arise because the bond for O to Al may have a more covalent character when the O is below the surface than when it is above the surface. We present evidence consistent with this view. An O adatom island with all the O atoms in threefold sites gives calculated O 1*s* BE's which are significantly higher for the perimeter O atoms. Further, the results for an isolated O island without the Al substrate present also give higher BE's for the perimeter atoms. Both these results are consistent with interpretation (b). Published scanning-tunneling-microscopy data supports the suggestion that the chemisorbed state consists of small, close-packed islands, whereas the presence of two vibrational modes in high-resolution electron-energy-loss spectroscopy data has been interpreted as representing surface and subsurface oxygen atoms. In light of the present results, we suggest that a vibrational interpretation in terms of interior and perimeter adatoms should be considered.

I. INTRODUCTION

The interaction of oxygen with single-crystal Al surfaces has been extensively studied in the past as a model oxygen-atom–free-electron metal system. Unfortunately it is not a simple system, since, as is often the case for oxygen-metal interactions, differing adsorption conditions (pressure, exposure, oxygen purity) and surface conditions (temperature, purity, number of defects) clearly result in significant differences in both adsorption kinetics and final products. The situation up to 1984 was reviewed by Batra and Kleinman,[1] particularly with respect to electronic structure theory and photoemission experiments. One of their conclusions was that oxygen bonded in at least two distinct sites prior to the later (greater exposure) formation of Al_2O_3, which is signaled in x-ray photoelectron spectroscopy (XPS) by an Al 2*p* chemical shift of ~ 2.7 eV compared to the metal.

Since then there have been a number of high-resolution electron-energy-loss spectroscopy (HREELS) vibrational studies,[2–5] some scanning-tunneling-microscopy (STM) work,[6] and a higher-resolution synchrotron Al 2*p* core-level study.[7] The consensus from the HREELS studies is that both *surface* and *subsurface* species are formed during adsorption at temperatures of 120 to 300 K prior to the formation of Al_2O_3. Cromwell, Chen, and Yates[3] concluded that both species were formed together, but that lower temperature and lower exposure favored the surface species, whereas higher exposure or annealing an exposed surface to higher temperatures favored the formation of the subsurface species. The actual identification of surface or subsurface oxygen species relies on the assignment of a vibrational feature between 545–650 cm^{-1} as an Al-O surface stretching mode and an 825–850 cm^{-1} feature as an Al-O underlayer mode. This assignment was made using parametrized force constant lattice dynamical calculations;[2] the uniqueness of these assignments, particularly for the "underlayer mode" must be questionable when based on such parametrized calculations. On the other hand, the onset of Al_2O_3 formation in the HREELS is easily recognized by a sharp, intense, three-peaked structure whose development coincides with the formation of the 2.7-eV shifted Al 2*p* core level in photoemission and a characteristic transition at 54 eV in the Auger spectrum.[3]

Astadi, Geng, and Jacobi[5] offer a somewhat different interpretation of very similar HREELS data. From earlier angle-resolved ultraviolet photoemission spectroscopy (ARUPS) work they had concluded that atomic oxygen islands must be formed for room-temperature adsorption. To make this consistent with the idea that the HREELS vibrational spectra represented surface and subsurface oxygen species they concluded that both *two-layer oxygen islands* (dominant at 300 K) and a *single-layer oxygen island* (dominant at 120 K) must be formed. Another significant point in this work is that conversion of the adsorbed species (whatever the correct structural assignment) into Al_2O_3 was observed as a function of time after adsorption at both 120 and 300 K, as demonstrated by the decrease in intensity of the adsorbate vi-

brational modes and the growth of the oxide features. Finally, adsorption at 20 K showed that penetration of the surface to form oxide nuclei occurred early and rapidly with almost no tendency to form the adsorbate structures first.

The synchrotron photoemission study of McConville *et al.*[7] revealed that prior to the formation of the Al $2p$ chemically shifted peak at 2.7 eV, representing Al_2O_3, three other discrete shifts could be identified at 0.49, 0.97, and 1.46 eV. The authors proposed that these represented conditions where Al atoms were coordinated to one, two, and three O atoms, respectively, prior to the formation of Al_2O_3 where Al has 4–6 coordination depending on the structure (crystalline or amorphous). The exposure evolution and decay of these peaks was compatible with this interpretation. In our opinion, these results may also be compatible with the growth of oxygen islands from an initial situation of isolated atoms, through smaller oxygen islands up to larger oxygen islands. Obviously the average O-Al coordination changes during the process and could cause such differences in the Al $2p$ chemical shift.

Finally, a brief STM report[6] shows that on flat Al(111) terraces adsorption at room temperature between about 5–30 % monolayer coverage resulted in imagable close-packed O islands some 7–20 Å in diameter. One cannot be sure from the STM results whether they represent single- or double-layer islands, but one can be sure that under these conditions [starting with large Al(111) terraces free of O contaminant] only this *one* type of chemisorbed species forms in addition to oxide nucleations. Annealing to higher temperatures causes the islands to grow, as does increasing exposure. In the absence of steps, poorly annealed regions, or O impurities left during cleaning, it is possible to almost cover the terraces with these islands *before* significant oxide nucleation starts.

There is thus a direct contradiction between the interpretation of the HREELS vibrational data and the STM data. The vibrational data has been interpreted as representing the formation of surface and subsurface chemisorbed O species (or, alternatively, single-layer islands and double-layer islands) with a conversion of the former to the latter by increasing the temperature or exposure occurring prior to oxide nucleation, whereas the STM results indicate only one type of close-packed oxygen island, which grows in size on annealing or increasing exposure. The high-resolution Al $2p$ chemical shift results can easily be considered consistent with the island growth interpretation, but we do not rule out that they may also be consistent with a surface and subsurface species interpretation.

In the present work we have tried to resolve the question of whether the chemisorption stage consists of *two* O species, one on the surface and one below, or of growing close-packed O islands, by directly examining the behavior of the O $1s$ core level. Experimentally, we have examined the O $1s$ XPS as a function of exposure, time after exposure, and detection angle to vary the surface sensitivity of the measurement. Theoretically, we have performed *ab initio* electronic-structure calculations using Hartree-Fock, self-consistent-field (SCF) wave functions for various clusters of Al and O atoms used to model the Al(111)/O interaction. The O $1s$ binding energy (BE) is calculated, within the constraints of Koopmans's theorem,[8,9] as the inverse of the one-electron orbital energies. We are primarily interested in the *differences* of the O $1s$ BE's for O atoms in various geometric positions. We expect that the use of Koopmans's theorem, which neglects the relaxation energy in response to the core hole, is a satisfactory procedure to obtain these differences.[9] This is the case because the relaxation energy depends dominantly on the overall size of the system and only secondarily on the specific geometrical position of the core ionized atom. For the present case, we have explicitly confirmed this expectation through the direct calculation of the relaxation energy for one of the clusters used to model Al(111)/O.

II. EXPERIMENT

The electron spectrometer used has been previously described.[10] The base pressure obtained during this work was 1×10^{-10} Torr. Al $K\alpha$ and He II photon sources were used (1486.6 and 40.8 eV, respectively). The hemispherical analyzer was used at a resolution corresponding to a 0.9-eV line (full width at half maximum) for the Ag $3d_{5/2}$ peak using the unmonochromatized Al $K\alpha$ source. The Al(111) crystal (cut and polished to within 0.6°) was electropolished and then cleaned *in situ* using Ar^+ bombardment and annealing cycles until the O $1s$ and C $1s$ impurities dropped below detectable limits. No other impurities were detected. Oxygen was introduced, from a separate UHV line, through a beam doser consisting of a capillary array directly onto the crystal from a few mm distance. The dosing lines were flushed with oxygen many times prior to the adsorption run in order to minimize contaminants and wall reactions (especially the presence of water). XPS spectra of Al $2p_{3/2}$ and O($1s$) were taken at electron-take-off angles between 10° and 80° to vary the surface sensitivity of the measurements. The He II spectrum of the valence-band region was recorded at 10°. The spectrometer BE scale was calibrated against the clean Al Fermi edge, determined from the He II spectrum.

III. XPS RESULTS AND DISCUSSION

Figure 1 shows the Al $2p$ and O $1s$ spectra for the clean surface and after exposure at 300 K, to about 100 L of oxygen (3×10^{-7} Torr for 330 sec); the spectra are for take-off angles of 80°, near normal exit, and 10°, grazing exit. Based on the relative O $1s$/Al $2p_{3/2}$ intensities, the known photoionization cross sections,[11] and an electron escape depth for the Al $2p_{3/2}$ electron through Al of ~27 Å,[12] the coverage achieved is estimated to be ~0.3 monolayer. A monolayer is defined as one oxygen atom per surface Al atom. The main points to note are that two O $1s$ features are observed, at ~532.1 and 533.5 eV; that the ratio of the 533.5/532.1-eV peaks increases at the more surface-sensitive angle; and that *no* change in the Al $2p_{3/2}$ peak shape is observed with oxygen adsorption, even at the more surface sensitive 10° angle.

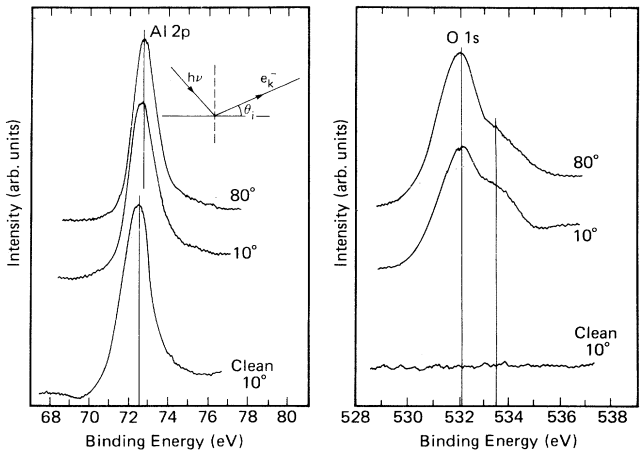

FIG. 1. Al 2*p* and O 1*s* XPS spectra for a clean Al(111) surface and after oxygen adsorbed at 300 K with a coverage of 0.3 ML. The measurements were performed at a take-off angle of 10° (grazing to the surface) and 80° (near normal to the surface). Noteworthy are the two components in the O 1*s* spectrum and the very similar shape of the Al 2*p* lines before and after the oxygen exposure.

Figure 2 shows the 10° spectra as a function of time after the oxygen exposure. The Al 2*p* peak does not change it shape or position, though there is a slight loss in intensity with time. The O 1*s* spectrum changes significantly with time; there is a loss of intensity in the higher BE peak and a corresponding growth in the lower one. There is not much change in the spectra after 30 min and they are completely stable after 60 min. The total intensities of the O 2*s* and Al $2p_{3/2}$ peaks did not change with time, within the accuracy of the data; ±10%. This indicates that there is no overall loss of oxygen from the Al surface within the XPS probing depth.

The O 1*s* data of Figs. 1 and 2 show that there are two

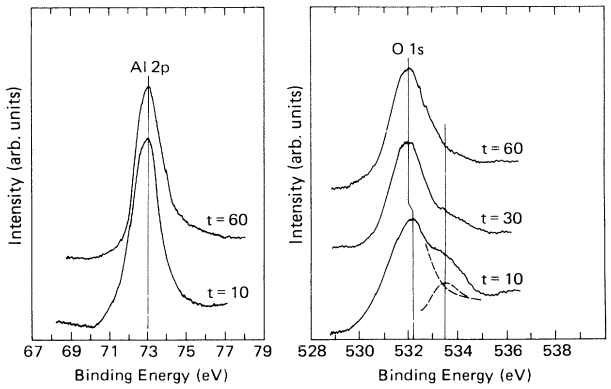

FIG. 2. Al 2*p* and O 1*s* spectra for oxygen adsorbed at 300 K with a coverage of 0.3 ML after 10, 30, and 60 min.

electronically different types of oxygen present for the ~100 L, 0.3 monolayer, atomic oxygen coverage situation. The Al 2*p* data show that at this coverage, under these exposure conditions, no significant oxide, Al_2O_3, has yet been formed. If it had, a 2.7-eV chemically shifted component would be observable in the 10° data. We are, therefore, still clearly in the chemisorption regime. The XPS literature of metal-oxygen is replete with cases where OH or CO_3 O 1*s* features have been misassigned to O adsorption,[13] so it is incumbent on us to consider these possible impurity species as candidates for the higher BE (533.5 eV) O 1*s* feature. A CO_3 species can be ruled out since no equivalent C 1*s* at 288–290 eV is found [the known region for surface carbonates on Ag (Ref. 14) and on Ni (Ref. 15)]. Elimination of OH adsorption as a candidate for the 533.5-eV peak is more difficult since it is known that the Al/OH O 1*s* comes at ~533 eV. Two pieces of evidence indicate that we do not have a problem of coadsorption of H_2O impurity leading to OH adsorption. First, leavig a clean surface in the spectrometer vacuum for 1 h does not produce any 533.5-eV feature and leaving it in vacuum for 1 h after exposure to O_2 decreases the 533.5-eV feature (Fig. 2). This is not a foolproof argument, since it is possible that any H_2O contaminant *only* reacts during O_2 exposure. The second piece of evidence is the He II generated valence-band spectrum of the 100-L exposed surface (not shown). The spectrum is consistent with previous valence-band studies on the Al/O systems and does not show any evidence of a peak at around 11 eV where the O-H σ band is generically expected. Since the He II spectrum is even more surface sensitive than the 10° XPS data, and OH adsorption cannot be detected, this seems to rule out an OH adsorption assignment for the 533.5-eV O 1*s* peak.

Having established that the 533.5-eV O 1*s* peak is unlikely to represent a contaminant there are two interpetations which can, in principle, explain our experimental data: (a) O adsorption on and below the Al surface, with the 533-eV peak representing the surface O and the 532.1-eV peak representing the subsurface O. The angular behavior is consistent with this and the conversion of the 533.5-eV peak to the 532.1-eV peak with time would correspond to O diffusion under the Al(111) surface. (b) O adsorption into *small,* isolated, O adatom islands, such that the perimeter atoms are sufficiently electronically different from the interior atoms to be represented by the 533.5-eV O 1*s* peak with the interior atoms as the 532.1-eV peak. The angular behavior is correct, because even with all the O atoms in the same plane the interior atoms of small, isolated, close-packed, islands will suffer greater self-attenuation at grazing-detection angles than will perimeter atoms. This attenuation will occur for reasonable take-off angles because the spatial extent of the O charge distribution, in particular in the direction normal to the surface, is roughly comparable to the O-O lateral spacing. The 533.5-eV feature could also represent essentially isolated O adatoms. The conversion of the 533.5-eV peak to the 532.1-eV peak with time then simply represents the growth of the two-dimensional (2D) islands and the incorporation of any single adatoms into them. Assuming round islands the number of perimeter atoms increases

linearly with the cluster radius whereas the interior atoms increase as the radius squared.

The effects of changing exposure, though not shown in Figs. 1 and 2, are also compatible with both explanations above: at lower exposures the *higher* BE O 1*s* feature is relatively more significant. At higher exposures it is less signficant.

IV. CLUSTER MODEL WAVE FUNCTIONS AND ANALYSIS

In order to distinguish the two interpretations which, as we discussed earlier, fit the experimental data, we have obtained *ab initio* SCF wave functions for several Al_nO_m clusters. Cluster models, especially those based on *ab initio* molecular orbital (MO) wave functions, have been used extensively to investigate and characterize the nature of the adsorbate-substrate interaction.[16] In particular, the MO cluster model has been used to analyze and correctly interpret both ultraviolet photoemission spectroscopy[17,18] (UPS) and XPS (Ref. 18) photoemission data for chemisorbed molecules. It is important to note that there is a broad base of experience to show that the results obtained with rather small cluster models are able to give qualitatively correct descriptions of many aspects of the interaction and bonding between adsorbates and surfaces.[19–21] We shall examine the effect of changing the number of atoms used to describe Al(111) on the 1*s* BE of an adsorbed O atom. This is done to prove that our conclusions reflect properties of the chemisorbed O and do not arise from size-dependent features of the cluster. In Sec. IV A, the theoretical framework for calculating binding energies is reviewed. In Sec. IV B, the results for the O 1*s* BE's or ionization potentials, IP's, for a single O atom either above or below the surface will be presented. (The terms BE or IP will be used almost interchangeably in this paper; in general, IP will be used in connection with discussions of basic aspects of the cluster model.) Also in Sec. IV B, details about the clusters used and the calculation of the SCF cluster wave functions will be given. In Sec. IV C, we present our theoretical results for the O 1*s* BE's for oxygen islands.

A. Theoretical framework for cluster IP's

We have used SCF wave functions for clusters modeling Al(111)/O to obtain the O 1*s* BE. For deep core levels, e.g., O 1*s*, SCF wave functions give reasonably accurate absolute values for the IP and give very good results for the shifts of the IP as the environment of the ionized atom changes.[9,22,23] Of particular importance is the fact that SCF wave functions permit the separation of initial- and final-state effects for the IP.

The IP's for ionization from an orbital ϕ_i can be obtained with a frozen orbital (FO) wave function, denoted $\Psi_i^{(n-1)}$(FO) for the ionic state; these IP's include initial-state effects only (Koopmans's theorem). This wave function is formed by removing an electron from ϕ_i but leaving all the orbitals unchanged with their initial-state character obtained for the SCF wave function for the ionized state, $\Psi^{(n)}$(SCF). The initial-state IP obtained with the FO ionic wave function is given as the difference between the energies of $\Psi_i^{(n-1)}$(FO) and $\Psi^{(n)}$(SCF); it is called the Koopmans's theorem IP and will be denoted here by KT BE or KT IP. If $\Psi^{(n)}$(SCF) is a closed-shell wave function, the KT IP is $-\varepsilon_i$, the SCF eigenvalue for the ionized orbital. If $\Psi^{(n)}$ (SCF) is an open-shell wave function, core ionization leads to different multiplet coupled states. In this case, $-\varepsilon_i$ is the weighted average of the KT IP's to these multiplets.[24,25] In the FO ionic wave function, screening, or relaxation of the passive orbitals, in response to the hole in ϕ_i is not permitted. However, it does include changes in the core-level IP which arise from the chemical environment of the ionized atom. To the extent that XPS core-level spectra reflect this environment, the initial-state KT IP's can give useful information.

In order to include the final-state relaxation or screening effects, it is necessary to obtain a SCF wave function for the ionic state, $\Psi_i^{(n-1)}$(SCF). The ΔSCF IP, given by $E[\Psi_i^{(n-1)}(\mathrm{SCF})]-E[\Psi^{(n)}(\mathrm{SCF})]$, does include the relaxation. The relaxation energy E_R is the difference between IP(KT) and IP(ΔSCF). The values of E_R are generally rather large; for the O 1*s* IP's in the clusters considered in this work, $E_R \sim 25$ eV. However, there is extensive evidence that E_R for the core-level ionization of an atom with a given nuclear charge is dominated by the size of the system which contains the ionized atom; see Ref. 9 and references therein. While E_R can be slightly different for different geometrical locations, or environments, of the ionized atom, this is normally of secondary importance compared to the size-dependent effect. Therefore, we will use the KT IP's for information about the changes in the O 1*s* IP for Al(111)/O due to changes in the geometrical environment of the ionized O atom. For one of the clusters with a single adsorbed O atom in positions both above and below the Al(111) surface, we have obtained both ΔSCF and KT 1*s* BE's. We have verified, and will show below, that the qualitative behavior of the shift of the 1*s* BE in these different positions is given by the Koopmans's theorem BE's.

B. O above and below the Al(111) surface

A threefold octahedral site is the most likely site through which an O atom can penetrate the Al(111) surface; there is no Al atom at this site until the third layer of Al. The O atom can bond above the surface and have three neighboring Al atoms. It can also bond below the surface, between the first and second layers; at this position, the O atom will have six neighboring Al atoms. The simplest Al cluster that we have used to model this site is Al_7(3,3,1) with three atoms in the first and second layers and one in the third layer; see Fig. 3(a). We have placed an O atom in the center of the threefold site to form Al_7O and varied the position of the O moving it from above to below the surface. We have also considered two larger Al clusters so that we could study the O 1*s* BE in different size clusters and so that we could represent an island of O atoms chemisorbed on Al(111). The Al_{19}(12,6,1) cluster is formed by adding nine first-layer and three second-

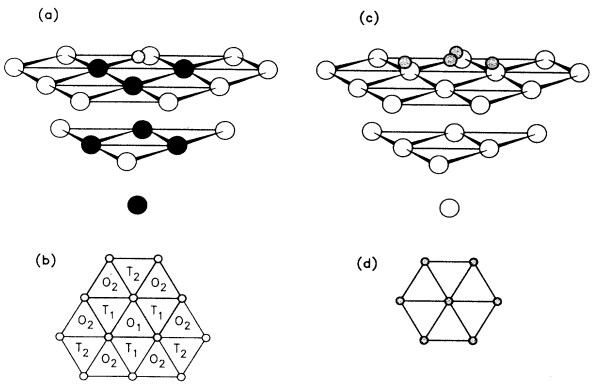

FIG. 3. Schematic vies of the Al_7O, $Al_{19}O$, $Al_{19}O_4$, and O_7 clusters. (a) Side view of the $Al_{19}O$ cluster. The O atom is shaded and the Al atoms are drawn as open and solid circles; the solid circles form the Al_7 cluster. (b) Top view of the 12 first-layer atoms of the Al_{19} cluster. The tetrahedral threefold sites are marked T_1 or T_2. The central octahedral threefold site is marked O_1 and the perimeter octahedral sites are marked O_2. (c) Side view of the $Al_{19}O_4$ cluster showing the closed-packed O_4 island with shaded circles. The four O atoms are at the sites labeled O_1 and T_1 in (b). (d) Top view of the O_7 cluster. The O-O geometry is such that the O atoms will occupy the sites labeled O_1 and O_2 in (b).

layer Al atoms to $Al_7(3,3,1)$; see Fig. 3(a). In Al_{19}, each of the three Al surface atoms which form the central, hexagonal, threefold site has the full ninefold coordination of an atom on the Al(111) surface, six in the first layer and three in the second layer. The $Al_{25}(12,6,7)$ is formed by adding the six third-layer atoms nearest the one third-layer Al atom in $Al_{19}(12,6,1)$. We also consider $Al_{19}O$ and $Al_{25}O$ clusters with O at the central threefold Al site and vary the O distance from the surface. For all the clusters, the Al-Al distances were kept at the bulk values; thus, an unreconstructed and unrelaxed surface was represented. Surface reconstruction will certainly change the specific values computed for properties of the chemisorption bond including, in particular, bond distance and bond energy. However, we do not expect that the reconstruction, unless it involves major and dramatic changes in the substrate geometry, will change the overall character of the Al—O bond and the behavior of the bond for different adsorbate geometries. Our goal is to use the cluster model to establish qualitative features and consequences of the Al—O bonding and we believe that the unreconstructed Al geometry allows us to do this.

The electronic structure of the clusters were obtained within the Hartree-Fock framework. *Ab initio* self-consistent field wave functions were calculated with basis sets of contracted Gaussian-type orbitals (GTO's); see Ref. 26 for a general description of the computational method. For Al_7 and Al_7O, all 13 electrons of Al were explicitly included in the SCF wave function. For the larger clusters, the Ne core of each Al atom was replaced with a nonlocal pseudopotential (PP), taken from Wadt and Hay;[27] only the three electrons arising from the atomic 3*s* and 3*p* shells were treated explicitly. This PP for Al was tested by comparing the all-electron results for Al_7O with those obtained with the Al PP for the same cluster. As shown below, the O 1*s* BE's were nearly the same for the two cases. For all clusters, O was treated as an all-electron atom. A flexible basis set[28] able to give reasonable representations for neutral O and anionic O was used; this basis set contained 9*s* and 5*p* GTO's contracted to 4*s* and 3*p* basis functions. For the all-electron Al atom, the 10*s* and 6*p* GTO set of Roos and Siegbahn[29] was contracted with a general, unsegmented, contraction technique[30] to 4*s* and 3*p* functions. The contraction was chosen so that the Ne core of Al was represented with a minimal basis while the 3*s* and 3*p* shells were represented by two basis functions each. For the PP Al atoms, 3*s* and 3*p* GTO's were contracted to 2*s* and 1*p*.[27] The SCF wave functions were computed using the C_{3v} symmetry of the clusters. The neutral initial states were determined by finding the single open-shell configuration with the lowest energy. The multiplet splitting of the singlet and triplet O 1*s*-hole states that arise from the coupling of the singly occupied 1*s* core level to the partially filled valence shell in the Al_nO clusters is not physically significant; it occurs because of the cluster size. For this reason, we have used $-\varepsilon$ (O 1*s*) for the O 1*s* KT BE; this choice represents ionization to a weighted average of the multiplet split ionic states.[24,25] For the SCF wave functions for the O 1*s*-hole states of Al_7O, we have used closed-shell Al_7O^- as the initial state to avoid the nonphysical final-state multiplets.

For the Al_7O all-electron wave functions, two energy minima were found. One minimum was for O 0.67 Å above the surface and the other for O 1.44 Å below the surface. Stohr *et al.*[31] concluded, based on extended x-ray absorption fine structure (EXAFS) measurements, that adsorbed O was 0.70(+0.10−0.15) Å above Al(111). We do not expect SCF wave functions for our relatively small clusters to give quantitative values for adsorbate geometries. However, the fact that even our smallest, Al_7O, cluster gives an Al-O distance reasonably close to the EXAFS value is an important indication that the SCF wave functions for Al_7O correctly describe the character of the Al—O bond. The almost exact agreement between the calculated and EXAFS values must be regarded as fortuitous.

The KT BE's for O at these equilibrium distances above and below the first layer of the Al(111) surface are given in Table I. The KT BE's are ~30 eV larger than the measured O 1*s* BE's at ~533 eV; this is because the KT values do not include the relaxation energy. The BE for O below the surface is *larger* by 1.6 eV than the BE for O above the surface. The relaxation energy is included in the ΔSCF BE's which are also given in Table I. The E_R is large ~23 eV, but it differs by less than 2% for O above and below the Al surface. This is fully consistent with earlier results[9,32] which show that E_R depends much more on the number of atoms in the system than on the precise geometric position of the ionized atom. The ΔSCF BE's are also reasonably close to our measured BE values, especially if an ~5-eV work function is added to the measured values to reference them to vacuum. How-

ever, of most importance, the ΔSCF BE for the O atom below the surface is still significantly larger, by 1.2 eV, than the ΔSCF BE for the O atom above the surface. Both the ΔSCF and KT BE's for the Al_7O cluster show that the O atom below the Al surface has a larger O 1*s* BE. This shift of the BE is not restricted to O atoms at their equilibrium positions above and below the surface. In Fig. 4 we show the O 1*s* KT BE for Al_7O as a function of the distance z of O from the Al surface. The O 1*s* BE increases monotonically from a distance well above the outer equilibrium to a maximum at $\simeq 1.2$ Å below the surface almost at the inner equilibrium, $z_e = -1.4$ Å. The increase of the KT O 1*s* BE between $z = +1.2$ Å and the maximum at $z = -1.2$ Å is almost 3 eV.

This is the opposite of the BE shift required for explanation (a) for the O 1*s* doublet seen in the XPS spectra. The relative intensity of the lower BE O 1*s* peak in the XPS spectra increases with an increase in emission angle, with O exposure, and also with time after exposure of Al to O. Thus, explanation (a) relates the lower BE peak to O atoms which have diffused below the surface. The Al_7O cluster calculation, however, shows that a subsurface O atom has a *larger* O 1*s* BE. This calculated shift is also opposite to the shift expected on the basis of arguments[32–35] about the coordination of the O atom above and below the surface. The coordination of the core-ionized atom plays an important role for the BE of atoms in metal clusters[32,33] and for the BE of bulk and surface atoms in crystals.[34] The diffuse "conduction-band" charge density surrounding the ionized atoms acts to lower the core-level BE. Since this charge density is greater when the coordination is greater, there is an initial-state effect which makes the core-level BE's of higher coordinated atoms smaller. This has been shown to be a dominant effect for simple metals[32–34] like Li and Al and it should also apply to O. The O atom above the surface is threefold coordinated to Al while the atom below the surface is sixfold coordinated to Al. Thus, the charge-density argument summarized above suggests that the O atom below the surface will have a smaller 1*s* BE in contradiction to the calculations. However, the charge-density argument assumes that the bonding character remains essentially the same for ionized atoms with different coordination. If the bonding character changes for atoms with different coordination, the BE shift will not be determined only by the coordination.

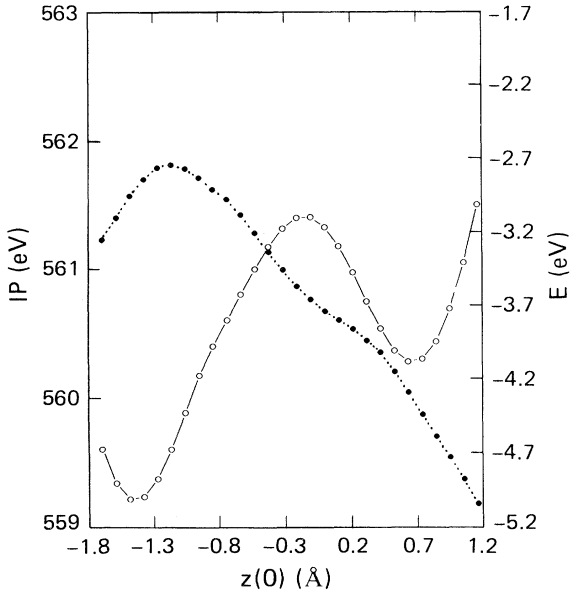

FIG. 4. Potential-energy curve, open circles, and KT O 1*s* IP, solid circles, as a function of the position of oxygen, z(O), above and below the surface for the Al_7O cluster. The potential energy is given with respect to the energy of Al_7^+ and O^- as zero.

TABLE I. O 1*s* BE's, in eV, for the Al_7O, $Al_{19}O$, $Al_{19}O(T)$, and $Al_{25}O$ clusters. The BE's are given for O at positions both above and below the Al surface. For Al_7O, the BE's are obtained in several ways; BE's for all-electron and PP wave functions are compared and KT and ΔSCF BE's are compared.

	O above Al	O below Al	Δ
Al_7O–all electron[a]			
KT	560.0	561.7	+1.6
ΔSCF	537.3	538.4	+1.2
E_R	22.8	23.2	
Al_7O–PP[b]			
KT	560.4	561.9	+1.5
$Al_{19}O$[c]			
KT	560.6	562.6	+2.0
$Al_{19}O(T)$[d]			
KT	560.3		
$Al_{25}O$[e]			
KT	560.7	562.3	+1.6

[a]The BE's are for O near $z = +0.67$ and -1.44 Å; these are the calculated z_e for O above and below Al with the all-electron Al_7O wave functions.
[b]The BE's are for O near $z_e = +0.76$ and -1.45 Å; the calculated z_e for the PP Al_7O wave functions.
[c]The BE's are for O near $z_e = +0.66$ and -1.18 Å; the calculated z_e for $Al_{19}O$.
[d]The BE is for O at $z = 0.66$ Å.
[e]The BE's are for O near $z_e = +0.56$ Å and at $z = -1.30$ Å. The equilibrium z for O below Al_{25} was not obtained.

The dipole moment curve for μ_z of Al_7O as a function of the position z of the O atom from the Al surface is shown in Fig. 5. (For the C_{3v} Al_7O cluster, μ_z is the only nonzero component of the cluster dipole moment.) The complicated curve of Fig. 5 gives evidence that the Al—O bond is not a simple ionic bond and that it may well be changing character as O moves below the surface. If the Al—O bond were ionic with negatively charged O, O^{-q}, we would expect the $\mu_z(z)$ curve to increase as z decreases and to be reasonably linear. This is the behavior which is found[35] for Cu(100)/O but it is not at all the behavior for Al(111)/O. In fact over a large distance, from

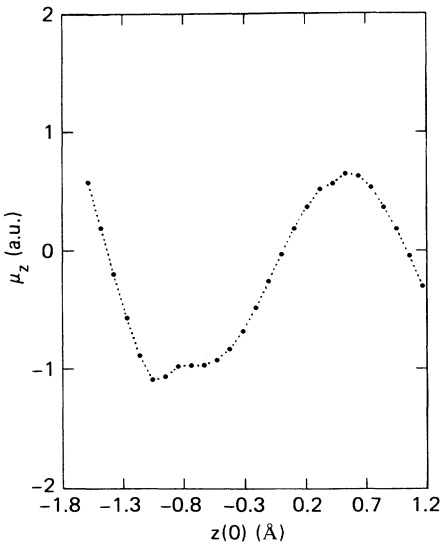

FIG. 5. Dipole moment curve for μ_z as a function of the position of oxygen, z(O), above and below the surface for the Al_7O cluster. The dipole moment is in a.u., 1 a.u. = 2.54 D.

$z \cong +0.6$ Å to $z \cong -1.0$ Å, the value fo μ_z decreases rather than increases. The decrease of μ_z over this range of ~ 1.5 Å is large, ~ 1.9 a.u. = 4.8 D. This behavior is consistent with a decrease of the ionicity q of O. It is possible to suppose that O is reasonably anionic well above the surface; note the linear behavior of $\mu_z(z)$ between $z = \sim +1.2$ to $\sim +0.6$ Å, but that as it approaches and goes below the Al(111) surface, its ionic character decreases. This decrease could be compensated by an increase in the covalent character of the Al—O bond. Such a change of bonding character would certainly be consistent with the large decrease of μ_z from $z \cong +0.6$ to -1.0 Å. It could explain why there is an increase in the O 1s BE as O moves lower even though its coordination by Al atoms increases. Norman *et al.*[36] have made arguments about the differences in the O ionicity for chemisorbed oxygen and for various oxide phases in order to explain the Al—O bond lengths deduced from their EXAFS measurements. For O chemisorbed above the surface, they argue that there is considerable covalent character in the Al—O bond. This is consistent with the fact that our dipole moment curve for Al_7O is not at all linear near the equilibrium bond distance above the surface of $z_e = 0.67$ Å; see Fig. 5. For a situation which they model by an ordered oxygen structure below the Al surface, they conclude that O below the surface is more ionic than chemisorbed oxygen above the surface. This is not consistent with our discussion above although we have considered only an isolated O atom rather than an ordered structure. However, the conclusions of Norman *et al.*[36] are based on an assumed relationship between the O ionicity and the Al—O bond length which may be an oversimplification. On the other hand, our argument is based on the dipole moment curve which is obtained from the electronic wave function and, hence, is directly related to the character of the Al—O bond.

The detailed character of the complex Al—O bond requires further study. While an increase in the covalency and a decrease in the ionicity of the Al—O bond as O moves below the surface is plausible, it has not been proven. Note, however, that Al_2O_3 is considered to be a covalent oxide, compared to the ionic transition metal oxides, such as NiO or CuO.

Similar differences between the O 1s BE's above and below the Al(111) surface have also been found with the larger $Al_{19}O$ and $Al_{25}O$ clusters; see Table I. The KT 1s BE for O below the surface is larger by 1.6 and 2.0 eV, respectively, for $Al_{19}O$ and $Al_{25}O$. For these clusters, we have used a PP for the Ne cores of the Al atoms, see above. We tested the PP to verify that it did not induce signficant artifacts or errors in the cluster calculations by comparing the PP and all electron results for the Al_7O cluster, see Table I. There are some differences between the z_e for the two cases. With the PP for Al_7O, the energy minima for O are at $z_e = +0.76$ and -1.45 Å; in particular, the PP z_e for O above the surface is 13% larger than the z_e in the all-electron case. The smaller Al valence-shell, 3s and 3p region, basis set for the PP calculations than for the all-electron calculations may explain, in part, the difference in z_e above the surface. However, at the PP z_e, the KT O 1s BE for Al_7O is essentially the same as for the all-electron (AE) calculation; this is true both for the absolute values of the BE's and for the differences between the BE's for O above and below the surface. The very similar PP and AE results for the O 1s BE's for Al_7O give us confidence in the PP results for $Al_{19}O$ and $Al_{25}O$. In summary, the O 1s BE for an O atom at an octahedral threefold site above Al(111) is significantly smaller than the BE for an O atom below the surface. This is an initial-state effect; the difference of the BE's is not changed greatly when final-state relaxation effects are included with ΔSCF BE's. This shift is consistently found for all the size Al clusters which were used to model the Al(111) surface. We tentatively assign the effect to O above the surface being largely ionic in character and O below the surface being substantially covalent.

It is possible, although unlikely, that the 1s BE of an O atom adsorbed at a tetrahedral threefold site of Al(111) could be significantly different from that for an O at an octahedral site. In order to investigate this possibility, we placed an O atom above Al at a tetrahedral site of Al_{19}. There are two inequivalent sets of tetrahedral sites for Al_{19}, marked T_1 and T_2 in Fig. 3(b). An O atom was placed at $z = 0.66$ Å, the z_e for the octahedral site of $Al_{19}O$, at one of the T_1 sites to form the $Al_{19}O(T)$ cluster. The $Al_{19}O(T)$ cluster has only C_s point-group symmetry compared to the C_{3v} symmetry of $Al_{19}O$ for O at the octahedral site. The KT O 1s BE for $Al_{19}O(T)$ is 560.3 eV, only 0.3-eV smaller than the BE at the octahedral site. In some part, cluster edge effects may have contributed to the small difference between the BE's at these sites. However, the important conclusion is that there is only a small difference between the O 1s BE at tetrahedral and octahedral threefold sites of Al(111). This small

difference cannot account for the ~1.4-eV difference for the two peaks observed in the XPS spectra.

The 1*s* BE of an O atom below the surface of Al(111) is ~1.0–2.0 eV *larger* than the 1*s* BE of an O atom above the surface in either an octahedral or a tetrahedral threefold site. This is overwhelmingly clear from all the results discussed above. We are, therefore, certain that the two O 1*s* experimental peaks *cannot* be ascribed to individual adsorbed O atoms located above and below the Al(111) surface.

C. O islands on Al(111)

The interior atoms in islands of adsorbed O atoms have a higher coordination than the perimeter atoms of the islands. This distinction might lead, following the arguments of Refs. 32–34, to lower core-level BE's for the higher coordinated interior atoms. The simplest island of O which has interior and perimeter atoms and which has the C_{3v} symmetry of the Al(111) surface has four atoms, three at the vertices of an equilateral triangle and one at the center of the triangle. For this "island," the central O atom is threefold coordinated by the perimeter O atoms at distance a. Each perimeter atom is onefold coordinated by the central atom; we do not count the other perimeter atoms of the triangle for the coordination because they are distant by $\sqrt{3}a$. We have formed the $Al_{19}O_4$ cluster, Fig. 3(c), by placing the O_4 island above Al_{19} with the central O above the central, octahedral, site. The perimeter O atoms of O_4 are at adjacent tetrahedral sites, labeled T_1 in Fig. 3(b). The plane of O_4 is parallel to the Al(111) surface and fixed at $z=0.69$ Å above the surface, close to z_e for $Al_{19}O$. In this geometry, the O atoms are very close together with a separation which is $1/\sqrt{3}$ of the Al-Al distance. The scanning-tunneling-microscopy (STM) experiments of Wintterlin *et al.*[6] and the EXAFS experiments of Stöhr *et al.*[31] indicate that (1×1) islands of O are formed with the O-O separation equal to the Al-Al separation. We shall consider below effects related to increasing the short O-O distance for the O island in $Al_{19}O_4$. In order to separately study the efects of the O-O interaction, we have studied the isolated O_4 cluster keeping the O-O distance the same as in $Al_{19}O_4$. Finally, we have considered the correct O-O separation and geometry for (1×1) islands of O/Al(111) using an isolated O_7 cluster. This cluster contains an interior O atom at the center and six perimeter O atoms at the vertices of a hexagon, see Fig. 3(d); the interior atom is sixfold and the perimeter atoms are threefold coordinated. For O_7 we have set the O-O separation equal to the Al-Al separation on Al(111); on an Al surface, each atom of the O_7 cluster could occupy an octahedral threefold site. The SCF wave functions for $Al_{19}O_4$, O_4, and O_7 have been computed as described in Sec. IV B. For $Al_{19}O_4$, the KT O 1*s* BE's for the interior and perimeter O atoms are given in Table II.

There is charge transfer from Al to O which forms partially anionic adsorbed O, O^{-q}. Therefore, the 1*s* BE of O^{-q} will be decreased from that for neutral O. For O above Al in $Al_{19}O$, the KT O 1*s* BE is ~2.5 eV smaller than that for an isolated neutral O atom. The KT O 1*s* BE's for both the interior and the perimeter O atoms in $Al_{19}O_4$ are significantly smaller, by ~2–3 eV, than the O 1*s* BE for the single O atom in $Al_{19}O$. An additional decrease in the 1*s* BE for the O atoms in $Al_{19}O_4$ could arise because each adsorbed O^{-q} is surrounded by the charge distributions of near-neighbor anionic adsorbed O atoms. This could easily lead to a further decrease of the 1*s* BE by ~2.5 eV.

TABLE II. O 1*s* BE's, in eV, for the interior and perimeter O atoms in the $Al_{19}O_4$, O_4, and O_7 clusters. For the perimeter atoms, the BE's are in a very narrow O 1*s* "band."

	Interior O	Perimeter O	Δ
$Al_{19}O_4$[a]	557.3	558.7	−1.4
O_4	564.5	565.2	−0.6
O_7	562.0	563.3	−1.2

[a]The plane of the O_4 atoms is at $z=0.69$ Å above the surface of Al_{19}.

More importantly, there is a large difference between the 1*s* BE's of the perimeter and interior O atoms with the perimeter atoms having the *larger* BE. This is the direction to be expected from the arguments of Refs. 32–34 about the coordination-dependent decrease in BE due to the charge density of the surrounding O atoms. However, we stress that there are other chemical-bonding effects which may change the core-level BE's in different directions. We have seen, in Sec. IV B that these other effects are important for the shift of the O 1*s* BE's between above and below surface positions of a single O atom on Al. Our calculations show that the coordination effect due to the charge density on neighboring O atoms dominates for $Al_{19}O_4$; the lower coordinated perimeter O atoms have a larger 1*s* Be than the interior O atom. The size of the difference between the BE's of the perimeter and the interior atoms is similar to the experimentally observed BE difference. This must be fortuitous since the O_4 island is both too small and too close packed for there to be any quantitative correspondence with O islands on the surface. However, it is important that we predict a large increase, $\gtrsim 1$ eV, in the 1*s* BE of the perimeter atoms over the interior atom. This result is completely consistent with interpretation (b) of the experimental data that the higher O 1*s* BE arises from O atoms at the perimeter of an island.

If the difference between 1*s* BE's of the perimeter and interior atoms is due to the presence of O neighbors of the ionized atom, then this effect should also appear for an isolated O_4 cluster. The KT 1*s* BE's for this O_4 cluster with the same geometry and O-O distances used in $Al_{19}O_4$ are given in Table II. The absolute vaues of the BE's are ~7 eV higher than for $Al_{19}O_4$. In part, this is because O_4 in $Al_{19}O_4$ has an effective negative charge coming from the charge transfer from Al while the isolated O_4 cluster is neutral. However, the KT 1*s* BE's for O_4 are larger than the equivalent KT value, $-\varepsilon(1s)=562.6$, for an isolated O atom. The larger values in O_4 arise from the chemical bonding of the O atoms to each other.

The possiblity of an increase can be understood in the valence-bond (VB) theoretical framework. The VB wave function for a molecule is a resonance of structures with neutral and with positively and negatively charged atoms. In a VB analysis, the O 1*s* BE of an atom in O_4 is the weighted average of the BE's for the differently charged O atoms in these resonance structures. This average can be larger than the BE for neutral oxygen because the increase in the 1*s* BE due to the removal of an O 2*p* electron to form O^+ is considerably larger than the decrease of the 1*s* BE due to the addition of an electron to form O^-. However, despite the overall increase in the KT O 1*s* BE's for O_4 over $Al_{19}O_4$, the difference between the BE's for the perimeter and interior atoms in O_4 is still large and in the same direction as for $Al_{19}O_4$. The BE's of the perimeter O's in O_4 are 0.6 eV *larger* than the BE of the interior O atom.

Finally, we examine the O-O coordination effect on the 1*s* BE between the sixfold coordinated interior and the threefold coordinated perimeter atoms of O_7. Here, the O-O distances are those for a (1×1) island on Al(111) and the actual size of the O_7 cluster is not much smaller than some of the islands observed directly[6] with the STM (7–20 Å). For O_7, there is also a large difference between the 1*s* BE's of the perimeter and the interior atoms. The 1*s* BE's of the perimeter atoms are 1.2 eV larger than the 1*s* BE of the interior atom.

To summarize this section, we have found that a significant O 1*s* BE distinction exists between interior and perimeter O atoms in small oxygen islands. This is found for all the clusters that we have used to simulate O islands, $Al_{19}O_4$, O_4, and O_7. Hence this result is *qualitatively* independent of the type of cluster used to simulate the island. *Quantitatively* the effect varies by about a factor of 2 with change in cluster conditions. The perimeter O atoms always have the *higher* BE.

V. CONCLUSIONS

We have shown that, whereas the two O 1*s* BE's observed in the chemisorption regime for Al(111)/O are experimentally consistent with an interpretation of the existence of surface and subsurface O atoms *or* the presence of small oxygen islands, only the latter interpretation is consistent with the cluster calculations performed to model the O 1*s* BE behavior. The model results are qualitatively independent of the details of the cluster and quantitativley within a factor of 2 of the experimental results. Our conclusion is that in the chemisorption regime of up to ~0.3 mL coverage at 300 K small, closed-packed, oxygen islands are the predominant product. From the ratio of the intensities of the two O 1*s* XPS peaks we estimate that some 20–25 % of the O adatoms are in perimeter sites plus individual isolated adatoms. On a time scale of about 30–60 min, the islands agglomerate and incorporate isolated atoms, and thus the perimeter fraction becomes very small, i.e., the islands grow considerably. This interpretation is in good agreement with a recent STM study[6] where on flat (111) terraces small (1×1) O islands were observed and no other species was seen prior to oxide formation. The interpretation is not in agreement with recent HREELS results,[2–5] however, where a particular vibrational frequency has been assinged to subsurface oxygen. It is not known whether this frequency could be reassigned to oxygen islands, but this should be considered.

As a general point for the interpretation of XPS O 1*s* data, there have been many misidentifications over the years of a second (or even a third) O 1*s* feature for metal/O interactions as representing chemisorbed O atoms in different geometric and/or electronic environments. Most have turned out to be different *chemical* species, such as OH, CO_3, CO, etc., and it has become tempting to dismiss *all* such claims as representing such impurities. In the light of the present results (particularly the calculations), it would seem unwise to do this. In particular, there is often evidence that for *initial,* low-coverage adsorption (~10% monolayer) an O 1*s* shoulder to high BE is preent. As coverage is increased it disappears or is swamped by the growing main peak. It is possible that this feature generically represents isolated O adatoms and perimeter atoms of very small islands.

*Permanent address: Departament de Química Física, Facultat de Química, Universitat de Barcelona, E-08028 Barcelona, Spain.

†Permanent address: Centro Informazioni Stude ed Esperienze S.p.A., Materials Division, Via Reggio Emilia 32, Segrate (Milano), Italy.

‡Permanent address: Department of Chemistry, University La Sapienza, Piazzale Aldo Moro 5-00185, Rome, Italy.

[1]I. P. Batra and L. Kleinman, J. Electron Spectrosc. Relat. Phenom. **33**, 175 (1984).

[2]R. L. Strong, B. Furney, F. W. de Wette, and J. L. Erskine, J. Electron Spectrosc. Relat. Phenom. **29**, 187 (1983).

[3]J. E. Crowell, J. G. Chen, and J. T. Yates, Surf. Sci. **165**, 37 (1986).

[4]J. G. Chen, J. E. Crowell, and J. T. Yates, J. Chem. Phys. **84**, 5906 (1986).

[5]C. Astaldi, P. Geng, and K. Jacobi, J. Electron Spectrosc. Relat. Phenom. **44**, 175 (1987).

[6]J. Wintterlin, H. Brune, H. Hoger, and R. J. Behm, Appl. Phys. A **47**, 99 (1988).

[7]C. F. McConville, D. L. Seymour, D. P. Woodruff, and S. Bao, Surf. Sci. **188**, 1 (1987).

[8]T. Koopmans, Physica **1**, 104 (1933).

[9]P. Bagus, D. Coulbaugh, S. P. Kowalczyk, G. Pacchioni, and F. Parmigiani, J. Electron Spectrosc. Relat. Phenom. **51**, 69 (1990) and references therein.

[10]C. R. Brundle, IBM J. Res. **22**, 235 (1978).

[11]J. H. Scofield J. Electron Spectrosc. and Relat. Phenom. **8**, 129 (1976).

[12]M. P. Seah and W. A. Dench, Surf. Interface Anal. **1**, 1 (1979).

[13]C. R. Brundle and J. Q. Broughton, in *Chemisorption Systems,* edited by D. A. King and D. P. Woodruff (Elsevier, Amster-

dam, 1991), Vol. 3A.
[14]C. J. Campbell and M. T. Paffet, Surf. Sci. **143**, 517 (1984).
[15]R. J. Behm and C. R. Brundle, Surf. Sci. (to be published).
[16]See, for example, P. S. Bagus, G. Pacchioni, and C. J. Nelin, in *Quantum Chemistry. Basic Aspects, Actual Trends,* edited by R. Carbo (Elsevier, Amsterdam, 1989), p. 475.
[17]P. S. Bagus and K. Hermann, Phys. Rev. B **33**, 2989 (1986); Appl. Surf. Sci. **22**, 444 (1985).
[18]K. Hermann, P. S. Bagus, C. R. Brundle, and D. Menzel, Phys. Rev. B **24**, 7025 (1981); C. R. Brundle, P. S. Bagus, D. Menzel, and K. Hermann, *ibid.* **24**, 7041 (1981).
[19]K. Hermann, P. S. Bagus, and C. J. Nelin, Phys. Rev. B **35**, 9467 (1987).
[20]P. S. Bagus, G. Pacchioni, and M. R. Philpott, J. Chem. Phys. **90**, 4287 (1989).
[21]M. Seel and P. S. Bagus, Phys. Rev. B **28**, 2023 (1983).
[22]P. S. Bagus, H. Schrenk, D. W. Davis, and D. A. Shirley, Phys. Rev. A **9**, 1090 (1974).
[23]C. J. Nelin, P. S. Bagus, R. J. Behm, and C. R. Brundle, Chem. Phys. Lett. **105**, 58 (1984).
[24]K. Hermann and P. S. Bagus, Phys. Rev. B **16**, 4195 (1977).
[25]P. A. Cox, Mol. Phys. **30**, 389 (1972).
[26]H. F. Schaefer III, *The Electronic Structure of Atoms and Molecules* (Addison-Wesley, Reading, MA, 1972).
[27]W. R. Wadt and P. J. Hay, J. Chem. Phys. **82**, 284 (1985).
[28]P. S. Bagus and U. Wahlgren, Mol. Phys. **33**, 641 (1977).
[29]B. Roos and P. Siegbahn, Theor. Chim. Acta (Berlin) **17**, 209 (1970).
[30]R. C. Raffenetti, J. Chem. Phys. **58**, 4452 (1973).
[31]J. Stöhr, L. I. Johansson, S. Brennan, M. Hecht, and J. N. Miller, Phys. Rev. B **22**, 4052 (1980).
[32]C. J. Nelin and P. S. Bagus, in *Festkörperprobleme,* edited by P. Grosse, Advances in Solid State Physics Vol. 25 (Viewig, Braunschweig, 1985), p. 135.
[33]F. Parmigiani, E. Kay, P. S. Bagus, and C. J. Nelin, J. Electron Spectrosc. Relat. Phenom. **36**, 257 (1985); P. S. Bagus, C. J. Nelin, E. Kay, and F. Parmigiani, *ibid.* **43**, c13 (1987).
[34]P. S. Bagus, G. Pacchioni, and F. Parmigiani, Phys. Rev. B **43**, 5172 (1991).
[35]P. S. Bagus and F. Illas, Phys. Rev. B **42**, 10852 (1990).
[36]D. Norman, S. Brennan, R. Jaeger, and J. Stöhr, Surf. Sci. **105**, L297 (1981).